

Assignment 1

The Poisson type PDE is defined on the square domain $\Omega \in [0, 1]^2$ with Dirichlet boundary conditions:

$$\begin{aligned} -\nabla \cdot (\gamma \nabla u) &= f, & \forall (x, y) \in \Omega, \\ u(x, y) &= u_\Gamma(x, y), & \forall (x, y) \in \Gamma. \end{aligned} \quad (1)$$

The solution and diffusion coefficient are, respectively,

$$u(x, y) = e^y \sin \frac{\pi(e^x - 1)}{e - 1}, \text{ and, } \gamma(x) = \frac{\pi e^x}{e - 1}. \quad (2)$$

Using the method of manufactured solutions, the load is determined to be,

$$f(x, y) = - \left\{ u(x, y) \gamma (1 - \gamma^2) + 2\gamma \frac{\partial u(x, y)}{\partial x} \right\}. \quad (3)$$

1. Deriving the adjoint formulation for the PDE and the objective

$$\begin{aligned} (\psi, \mathcal{L}u)_\Omega &= - \int_\Omega \psi (\gamma u_{,i})_{,i} d\Omega \\ &= - \int_\Omega (\psi \gamma u_{,i})_{,i} d\Omega + \int_\Omega \gamma \psi_{,i} u_{,i} d\Omega \\ &= - \int_\Gamma \psi (\gamma u_{,i} n_i) d\Gamma + \int_\Omega (\gamma \psi_{,i} u)_{,i} d\Omega + \int_\Omega u (-\gamma \psi_{,i})_{,i} d\Omega \\ &= \int_\Gamma \psi (-\gamma u_{,i} n_i) d\Gamma - \int_\Gamma u (-\gamma \psi_{,i} n_i) d\Gamma + (u, \mathcal{L}^* \psi)_\Omega \end{aligned}$$

From the compatibility condition,

$$(\psi, \mathcal{L}u)_\Omega - (u, \mathcal{L}^* \psi)_\Omega = (\mathcal{C}u, \mathcal{B}^* \psi)_\Gamma - (\mathcal{B}u, \mathcal{C}^* \psi)_\Gamma, \quad (4)$$

$$\begin{aligned} \mathcal{L} &\equiv -\nabla \cdot (\gamma \nabla), & \mathcal{L}^* &\equiv -\nabla \cdot (\gamma \nabla), \\ \mathcal{C} &\equiv -\hat{n} \cdot (\gamma \nabla), & \mathcal{C}^* &\equiv -\hat{n} \cdot (\gamma \nabla) \\ \mathcal{B} &\equiv 1, & \mathcal{B}^* &\equiv 1. \end{aligned}$$

$$\mathcal{J}(u) = \int_{\Gamma_1} \beta \gamma (\hat{n} \cdot \nabla u) d\Gamma_1 \quad (5)$$

$$\mathcal{J}(u) = (g, u)_\Omega + (c, \mathcal{C}u)_\Gamma \quad (6)$$

$$= \underbrace{-(u, \mathcal{L}^* \psi - g)_\Omega}_I - \underbrace{(\mathcal{C}u, \mathcal{B}^* \psi - c)_{\Gamma_1}}_{II} + (f, \psi)_\Omega + (b, \mathcal{C}^* \psi)_\Gamma \quad (7)$$

Comparing Equation (5) to Equation (7), $g = 0, c = \beta$. Setting I, II to 0, the adjoint formulation of the PDE is stated as,

$$\mathcal{L}^* \psi = 0, \quad \forall x \in \Omega, \quad (8)$$

$$\mathcal{B}^* \psi = \beta, \quad \forall x \in \Gamma_1, \quad (9)$$

$$\mathcal{B}^* \psi = 0.0, \quad \forall x \in \Gamma \setminus \Gamma_1. \quad (10)$$

2. Implementing an adjoint consistent discretization for Equations (1) and (2).

The weak form of the primal PDE is,

$$-\int_{\Gamma} v (\gamma u_{,i} n_i) d\Gamma + \int_{\Omega} v_{,i} \gamma u_{,i} d\Omega = \int_{\Omega} v f d\Omega.$$

In order to achieve adjoint consistency, the Dirichlet boundary conditions have to be weakly imposed. The following terms,

$$-\int_{\Gamma} (\gamma v_{,i} n_i) (u - u_{\Gamma}) d\Gamma + \frac{\kappa}{h} \int_{\Gamma} (\gamma v) (u - u_{\Gamma}) d\Gamma,$$

are added to the weak-form to maintain **coercivity** (positive definiteness) and to weakly impose Dirichlet boundary conditions.

$$\underbrace{\int_{\Omega} v_{,i} \gamma u_{,i} d\Omega}_A + \underbrace{\sigma \int_{\Gamma} (\gamma v_{,i} n_i) u d\Gamma - \int_{\Gamma} v (\gamma u_{,i} n_i) d\Gamma + \frac{\kappa}{h} \int_{\Gamma} \gamma u v d\Gamma}_B = \underbrace{\int_{\Omega} v f d\Omega}_C + \underbrace{\sigma \int_{\Gamma} (\gamma v_{,i} n_i) u_{\Gamma} d\Gamma + \frac{\kappa}{h} \int_{\Gamma} u_{\Gamma} \gamma v d\Gamma}_D, \quad (11)$$

where $\sigma = -1$, and $\kappa = (p+1)^2$ with p being the order of the polynomial function space used in the discretization of both the test function $v \in \mathcal{V}$ and the trial function $u \in \mathcal{U}$. The primal problem was discretized using H^1 continuous quadratic ($p = 2$) Finite Elements and was solved using PyMFEM. The following integrators in PyMFEM,

$$A \equiv \text{DiffusionIntegrator},$$

$$B \equiv \text{DGDiffusionIntegrator},$$

$$C \equiv \text{DomainLFIntegrator},$$

$$D \equiv \text{DGDirichletLFIntegrator},$$

were used to generate the bilinear and linear forms respectively. The integrators B, D were only applied to the Dirichlet Boundary Faces. A mesh-convergence study revealed errors with higher than a second-order rate of convergence ≈ 2.92 , in the L^2 norm as shown in Fig.1.

3. Solving the discrete adjoint problem

In order to account for the weak imposition of Dirichlet Boundary conditions, we need to add a penalty term to the functional $\mathcal{J}(u)$. This objective functional in the continuous form is modified to,

$$\mathcal{J}(u) = \int_{\Gamma_1} \beta \left((\gamma \hat{n} \cdot \nabla u) + \frac{\kappa}{h} \gamma (u - u_{\Gamma_1}) \right) d\Gamma_1.$$

This integral is discretized as,

$$\mathcal{J}(u) = \left(u, \left(\beta, \gamma \hat{n} \cdot \nabla v + \frac{\kappa}{h} \gamma v \right) \right) - (1, (\beta u_{\Gamma_1}, \gamma v)).$$

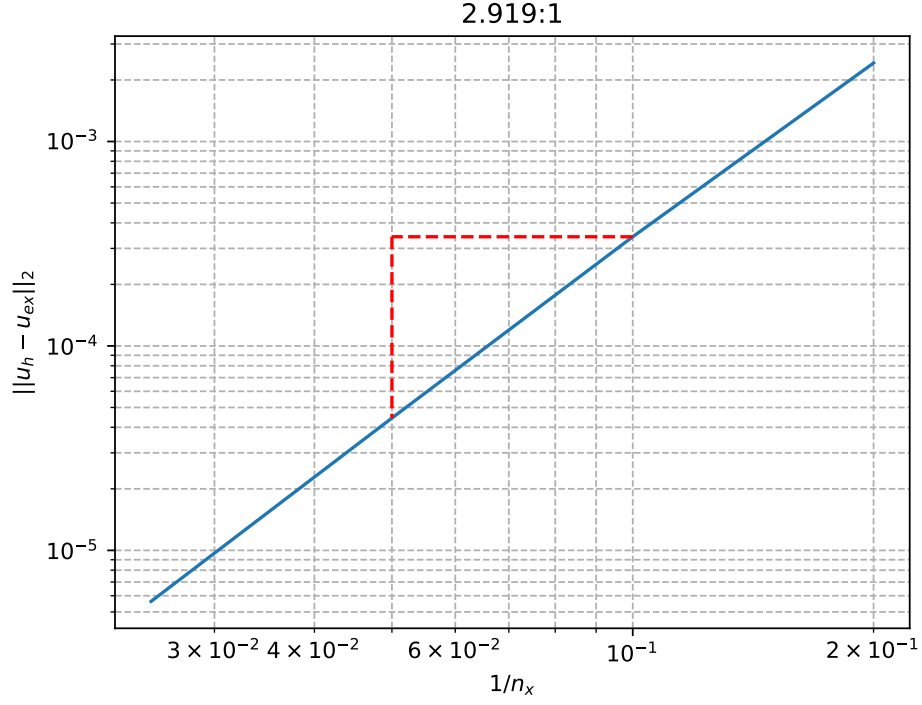


Figure 1: Rate of convergence of the L^2 solution error versus the mesh size n_x

This is achieved in PyMFEM by finding the inner product of the state variables u_h with the linear form g_h given by the numerical integration of the functional,

$$-\sigma \int_{\Gamma_1} \beta \gamma \hat{n} \cdot \nabla v \, d\Gamma_1 + \frac{\kappa}{h} \int_{\Gamma_1} \gamma v \, d\Gamma_1,$$

and adding it to the correction term given by the inner product of a vector of ones with the discretized numerical integration of the functional,

$$-\frac{\kappa}{h} \int_{\Gamma_1} \gamma u_{\Gamma_1} v \, d\Gamma_1.$$

Therefore, the discrete functional is given by,

$$J_h(u_h) = g_h^T u_h + \mathbf{1}^T c_h.$$

The Lagrangian of the discretized version of the primal problem is,

$$Lg(u) = g_h^T u_h + \mathbf{1}^T c_h + \psi_h^T (L_h u_h - f_h).$$

The discrete adjoint variables are calculated by setting,

$$\frac{\partial Lg}{\partial u_h} = L_h^T \psi_h + g_h = 0.$$

(a) Solving for the choice $\beta(x) = 1$

The contours of the discrete adjoint variables and the mesh convergence study of the error in functional computation is shown in Fig.2. This is not super-convergent because the adjoint variables are discontinuous at the boundaries $x = 0$ and $x = 1$ where $\beta(0) = \beta(1) = 1$ when technically it should have been 0.

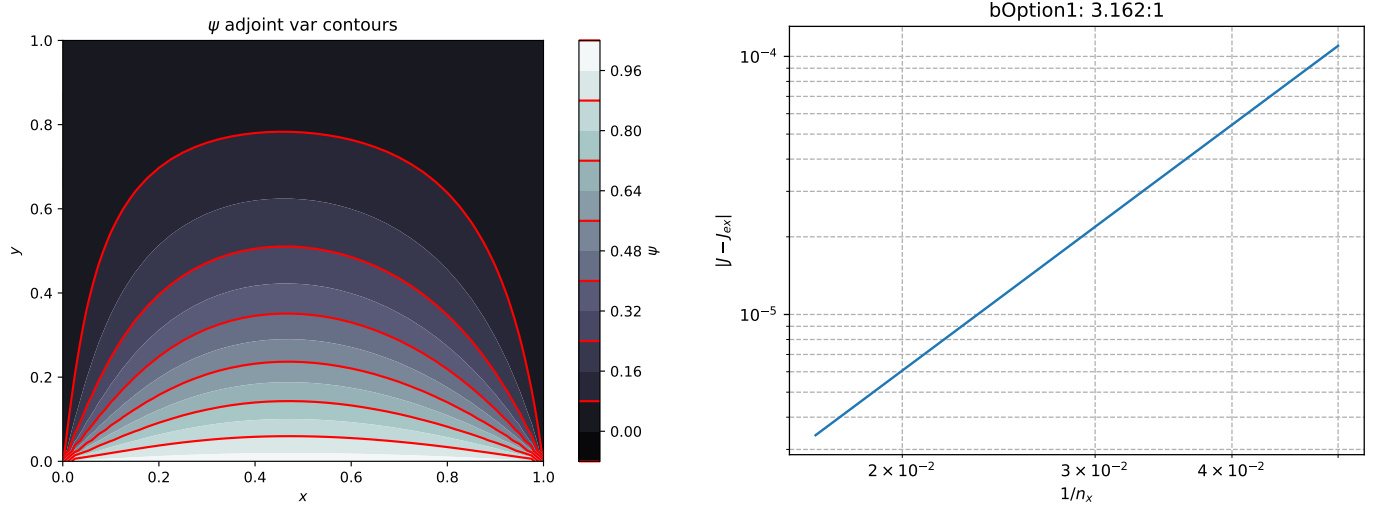


Figure 2: (a) Countours of the adjoint variables, (b) mesh convergence study of the functional error $|J - J_{\text{ex}}|$ versus mesh size $1/n_x$

(b) Solving for the choice $\beta(x) = \frac{\pi^2(e^x - 1)(e - e^x)}{(e - 1)^2}$

The contours of the discrete adjoint variables and the mesh convergence study of the error in functional computation is shown in Fig.3. This is super-convergent because the boundary

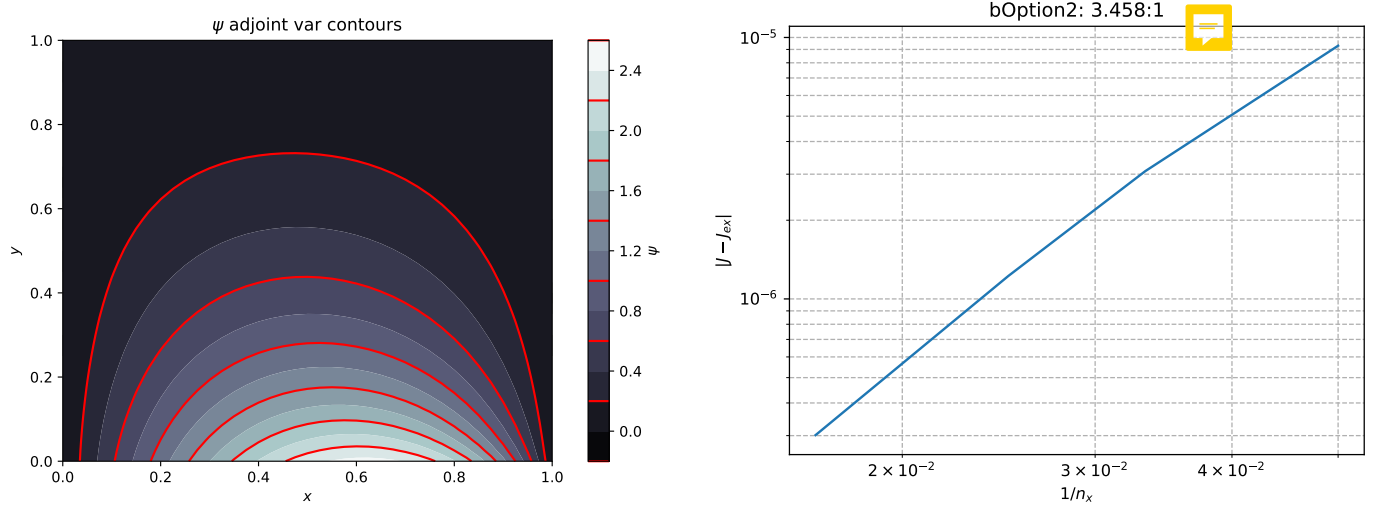


Figure 3: (a) Countours of the adjoint variables, (b) mesh convergence study of the functional error $|J - J_{\text{ex}}|$ versus mesh size $1/n_x$

conditions are not discontinuous at $x = 0$ and at $x = 1$ since $\beta(0) = \beta(1) = 0$.